PROCEEDINGS, 42nd Workshop on Geothermal Reservoir Engineering
Stanford University, Stanford, California, February 13-15, 2017
SGP-TR-212

Numerical Simulation of the Sumikawa Geothermal Reservoir, Japan, using iTOUGH2

Kenta Kondo[1], Ryuichi Itoi[1], Toshiaki Tanaka[1], Takaichi Iwasaki[2]

[1] Department of Earth Resources Engineering, Faculty of Engineering, Kyushu University, Fukuoka 819-0395, Japan

[2] Mitsubishi Materials Co., Tokyo, Japan

k-kondo@mine.kyushu-u.ac.jp

Keywords: reservoir simulation, numerical modeling, natural state simulation, history matching simulation, TOUGH2, iTOUGH2

ABSTRACT

A three-dimensional numerical model of the geothermal reservoir at the Sumikawa field was developed using inversion analysis with iTOUGH2 simulator. A sensitivity analysis for the reservoir rock type parameters (mainly permeability) was performed, and the priority of parameters to be estimated was determined through natural state simulation. After the sensitivity analysis was completed, inversion analysis was performed for the natural state and for a period of 20 years after the beginning of production activity. Rock permeabilities were estimated from measured temperature and pressure data in the natural state and from specific enthalpy and flow rate during production. Simulated temperatures and feed zone depth pressures in wellbores were compared with measurements to test goodness of fit. Simulated specific enthalpy during the production period was also compared with measurements using production and reinjection history matching.

1. INTRODUCTION

A numerical model is necessary for predicting geothermal reservoir behavior during production and reinjection operations and thus designing sustainable exploitation scenarios for the field. For this purpose, we first developed a numerical model of the Sumikawa reservoir for natural state conditions before any production activity was initiated. After natural state simulation, history matching was performed to match the simulated results of specific enthalpy of the production fluid with measurements. The Sumikawa geothermal field is located in Akita Prefecture, Japan, and the geothermal power plant has been operating with an installed capacity of 50 MWe since 1995. A numerical model of the Sumikawa geothermal field has been developed (Kato, 2003). We introduced new methods which quantitatively evaluate the simulated result using Root Mean Square Error (RMSE) and Relative Error (RE), and improved the numerical model using forward analysis, sensitivity analysis and inversion analysis with the TOUGH2 (Pruess et al., 1999) and iTOUGH2 (Finsterle el al., 2000) simulators.

2. NUMERICAL MODEL

In the Sumikawa geothermal field, the production area is located in the southern part of the field, and the reinjection area is located in the northern part, as shown in Fig 1. Well bottom locations are indicated by solid circles and their inclined trajectories by lines. Red, blue, and green circles denote production, reinjection, and observation wells, respectively.

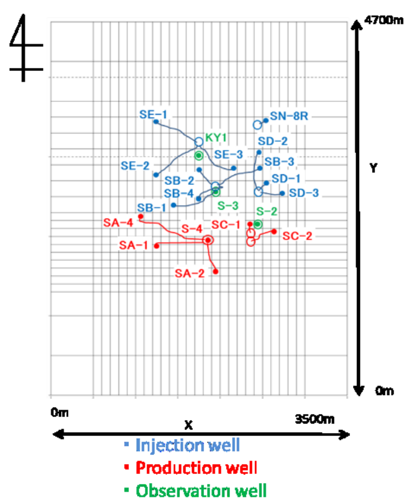

Figure 1: Well location on grid system

2.1 Grid System

A three-dimensional grid system of the Sumikawa geothermal reservoir is shown in Fig. 1. The grid system of the numerical model measures 3500m by 4700 m in the horizontal direction, and 3500 m in the vertical direction for elevations from −2500 m to 1000 m a.m.s.l. The grid size ranges from 100 m by 100 m to 500 m by 500 m. The model was divided into 20 layers in the vertical direction with different thickness ranging from 100 m to 300 m. The 20 layers commence with Layer A at the top and progress to Layer T at the bottom. There are a total of 10,852 grids in this model.

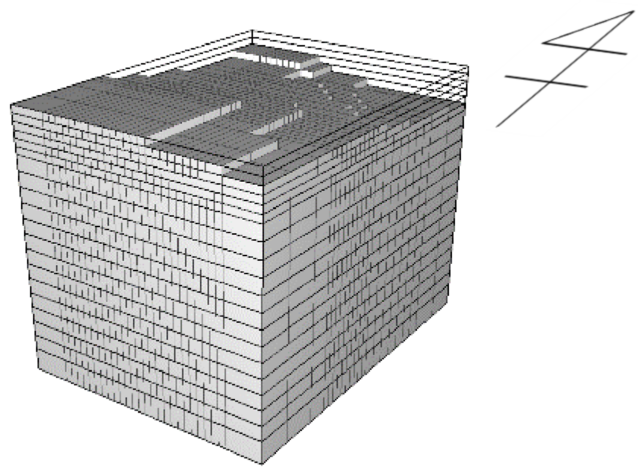

Figure 2: Three-dimensional grid model

2.2 Rock Properties

Table 1 summarizes the rock properties of each rock type. We assumed all rock types to be a porous medium. These rock properties (density, porosity, thermal conductivity, and specific heat) were taken from core analysis data.

Table 1: Rock properties

Rock type	Type	Porosity(-)	Density (kg/m^3)	Specific heat (J/kg/K)	Heat conductivity (W/m/K)
LLL11	POROUS	0.11	2640	1000	1.9
KKK11	POROUS	0.34	2690	980	2.9
FFF11	POROUS	0.15	2640	940	3.0
MVV11	POROUS	0.10	2660	910	3.3
MVV22	POROUS	0.10	2660	910	3.3
MVV33	POROUS	0.10	2660	910	3.3
MVV44	POROUS	0.10	2660	910	3.3
MVV55	POROUS	0.10	2660	910	3.3
BBB11	POROUS	0.04	2730	830	2.5
BBB22	POROUS	0.04	2730	830	2.5
BBB33	POROUS	0.04	2730	830	2.5
BBB44	POROUS	0.04	2730	830	2.5
BBB55	POROUS	0.04	2730	830	2.5
ZZZ11	POROUS	0.02	2710	750	3.0
ZZZ22	POROUS	0.02	2710	750	3.0
ZZZ33	POROUS	0.02	2710	750	3.0
XXX11	POROUS	0.15	2640	940	3.0

.

2.3 Initial and boundary conditions

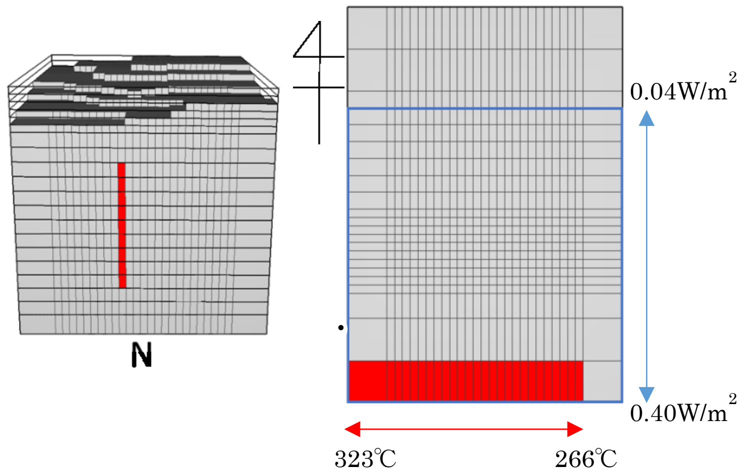

Figure 3: Discharge area in the lateral boundary (left) and mass flow and heat flux in the bottom layer (right)

We developed a numerical model using Petrasim software (Thunderhead Engineering, 2016) that includes TOUGH2 as a numerical simulator. For the initial conditions, a hydrostatic pressure profile saturated with water at 20°C was specified. As boundary conditions, a constant pressure of 0.0898 MPa, and temperature of 20°C above the top surface were given. The lateral boundaries were assumed to be impermeable to mass and adiabatic to heat. However, a discharge area was assigned to the north face in the lateral boundary in the red region as shown in the left figure of Fig. 3. Mass recharge and heat flux were assigned at the grid blocks as shown in the right figure of Fig 3. Mass recharge was specified at the grid blocks in red in the horizontal domain, and the total mass was 33.4 kg/s for temperatures of 266–323°C. Heat flux was specified for the grid blocks surrounded by the blue line, and was set at 0.04 W/m^2–0.40 W/m^2.

2.4 Hardware specification

In this study, we used the Intel Core i7-4771 CPU @ 3.50 GHz and the Intel HD Graphics 4600 GPU. This CPU has 4 cores and supports hyper-threading technology. Thus, it can process 8 threads in parallel.

3. FORWARD ANALYSIS AND INVERSE ANALYSIS

Figure 4 shows the flow chart of the analysis for this study. The procedure used for forward analysis and inversion analysis as shown in Fig. 4 is now explained:

The steps used in forward analysis were:

1) The numerical model (Fig. 1) was developed based on the conceptual model.

2) Rock properties, initial condition, boundary condition, and heat source were provided.

3) Natural state simulation was carried out using TOUGH2, and we compared the simulated results with measurements. If the results did not sufficiently correspond with the measured data, we changed the parameters (mainly permeabilities) and carried out the natural state simulation again.

4) After natural state simulation, history matching simulation was performed using TOUGH2. This simulation requires the result of natural state simulation as the initial condition. Then, we compared simulated results with measured data, mainly specific enthalpy. If the results did not provide a satisfactory match with the measured data, we changed the parameters and carried out the natural state simulation again.

5) We repeated this forward analysis until a satisfactory fit between measured and simulated results was obtained.

In forward simulation, the natural state before the commencement of production and reinjection operation (mainly temperature and pressure profiles) must be reproduced. History matching simulation should be conducted after natural state simulation is completed. In this simulation, production history, mainly specific enthalpy, should be represented. These simulations were both conducted using TOUGH2. The period of natural state simulation was 100,000 years, which is the period required for temperature and pressure stabilization in the reservoir domain. The initial conditions of temperature and pressure are given in section 2.3. The history matching simulation used the results of the natural state simulation as the initial temperature and pressure distribution conditions. The history matching simulation period was set to 20 years. We carried out history matching simulation using production and reinjection histories since 1994 when the production and reinjection started.

After forward analysis, we carried out inversion analysis for tuning parameter value more in detail. The procedures for inversion analysis are as follows:

1) Rock properties, initial condition, boundary condition and heat source were based on the results of forward analysis.

2) Rock properties (mainly permeabilities) were improved using iTOUGH2. Then, we changed permeabilities from initial guess (before estimation) to best estimated (after estimation).

3) Natural state simulation and history matching simulation were carried out using the same approach as forward analysis, including comparing the results with the measured data. We also compared the results of forward analysis and inverse analysis to verify the improvement in the results of inversion analysis.

4) If satisfactory matching with measured data was not achieved, we repeated the inversion analysis until satisfactory fitting was obtained.

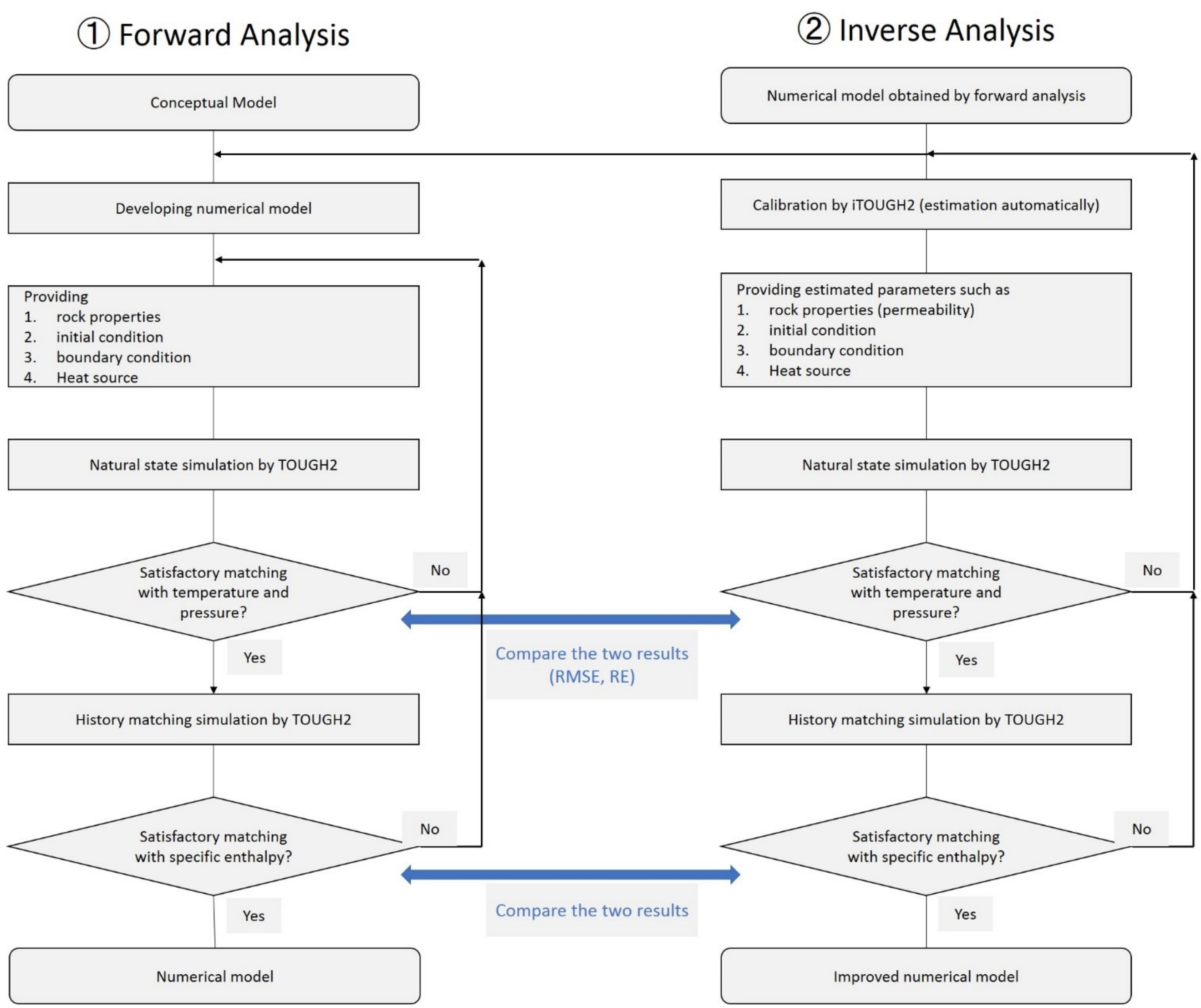

Figure 4: Flow chart of the analysis

.

In inversion analysis with iTOUGH2, an enormous computation time is required for the estimation process. Therefore, we first conducted a sensitivity analysis of the parameters to be estimated in the iTOUGH2 simulation, and extracted parameters with a large sensitivity, as shown in Fig. 5. From this sensitivity analysis, we found the most important parameters that influence the reservoir temperature markedly are the permeabilities of Rock type FFF11. Figure 6 shows the three-dimensional distributions of six rock types that are more sensitive than other rock types. Here, we denote that the estimated permeabilities through the forward analysis as the initial guess and through the inversion analysis as the best estimate. Table 2 summarizes the initial guess and best estimate.

Table 2: Initial guess and best estimates of rock permeability

Rock type	Initial guess ($10^{-15}m^2$)			Best estimate ($10^{-15}m^2$)		
	E-W	N-S	Vertical	E-W	N-S	Vertical
LLL11	2	2	2	2	2	2
KKK11	0.01	0.01	0.01	0.0001	0.0001	0.0001
FFF11	4	4	4	5.71	5.71	5.71
MVV11	0.5	0.5	0.5	1.18	1.18	0.49
MVV22	1	1	0.5	12.14	12.14	12.14
MVV33	40	40	5	68.3	68.3	6.83
MVV44	1	1	1	1.18	1.18	0.4
BBB22	20	20	1	59.19	59.19	0.45
BBB33	20	80	5	29.26	29.26	6.28
BBB44	1	1	1	3.45	3.45	1.09
BBB55	2	2	5	8.7	8.7	1.45
ZZZ11	20	20	20	1.5	1.5	1.5
ZZZ33	0.5	0.5	0.5	1.44	1.44	1.28

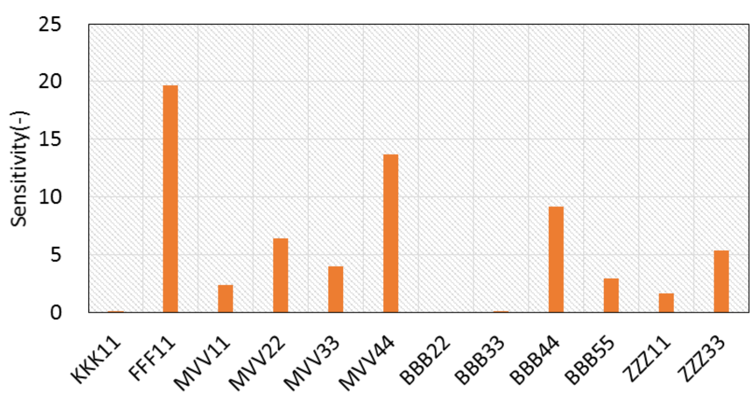

Figure 5: Sensitivity of permeability for each rock type

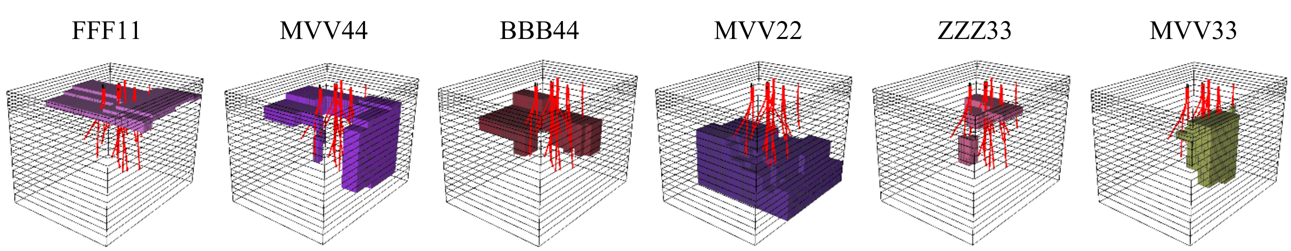

Figure 6: Three-dimensional distribution of each rock type (six examples)

3.1 Simulation results of the natural state

Figure 7 and 8 show the comparison between measured and simulated temperature profiles in the natural state in production wells and reinjection wells. Orange square and blue diamond indicate measurement and simulated results by the forward analysis, respectively. The simulated temperatures for wells SA-1 and SA-4 show good agreement with the measurements. Simulated temperatures for wells SC-1 and SC-2 also have a good fit with the measurements. However, the temperature of SC-1 and SC-2 showed discrepancies at depths greater than 0m a.m.s.l. There is a slight difference between the profiles of the calculated and measured temperatures in the reinjection wells. However, this result is acceptable because we estimated rock permeabilities mainly from measured temperature and pressure data in the natural state in the production wells.

Figure 7 and 8 also show simulated results for temperature using the best estimated permeabilities in the natural state. The black triangles denote simulated results using the best estimated permeabilities. A good agreement in the temperature profiles between simulated results and measurements was obtained in wells SA-1, SA-4, and SC-2. The temperature results in Well KY-1 were better than the results with the initial guess. However, these results still have large discrepancies. In contrast, the results for temperature profiles of wells SC-1, SB-1, and SB-3 remain unchanged when compared with the results before the inversion analysis.

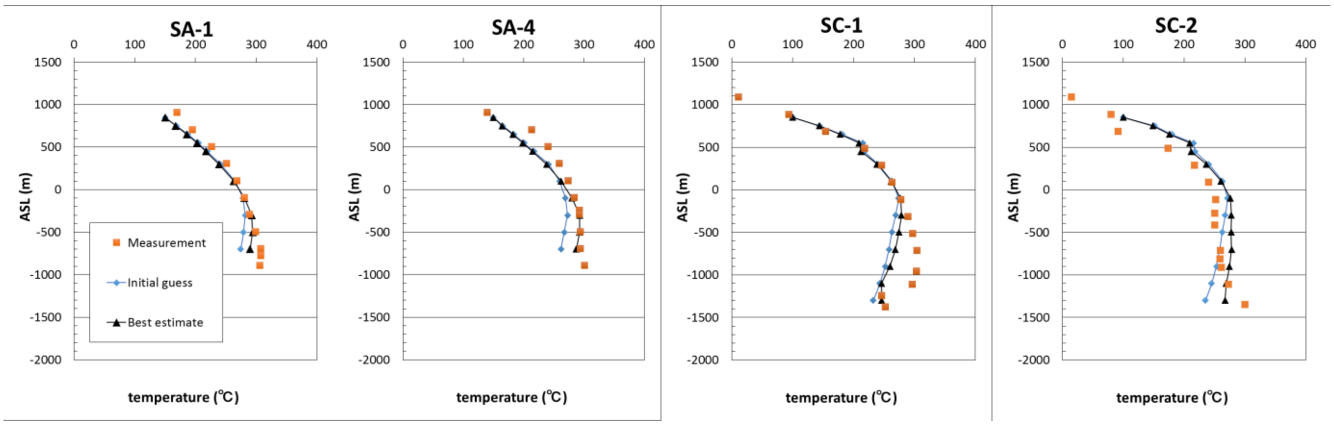

Figure 7: Temperature profile (the initial guess, the best estimate, and measured) in production wells

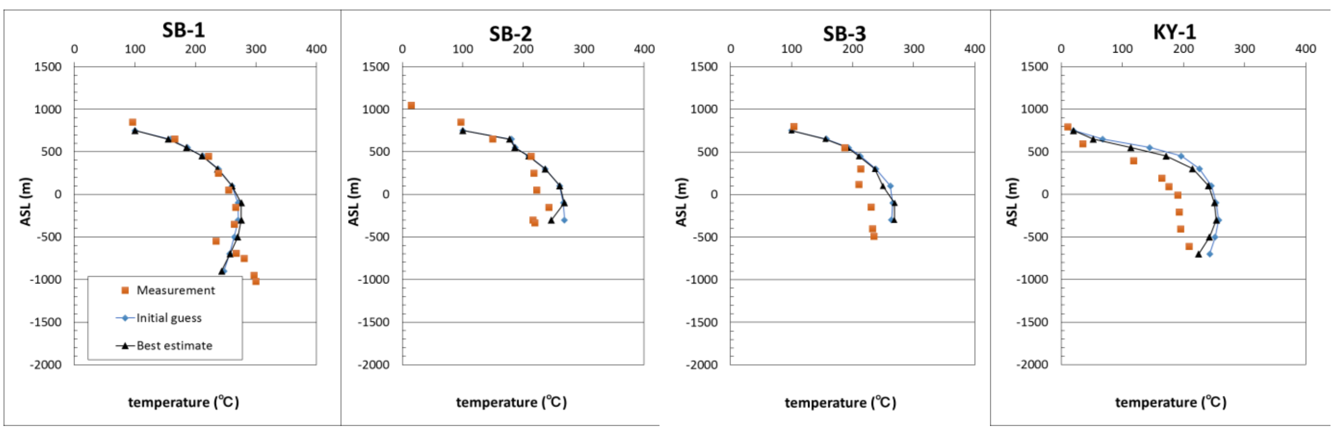

Figure 8: Temperature profile (the initial guess, the best estimate, and measured) in injection wells

We evaluated the difference between simulated results and measurements quantitatively using the root mean square error (RMSE). Figure 9 present the RMSE for simulated temperatures for initial guess and best estimate in the natural state simulation. It can be clearly seen that simulated results using the best estimate are better matches than the results using the initial guess. The RMSE was calculated using the following equation:

$$RMSE = \sqrt{\frac{1}{N}\sum_{i=1}^{N}(T_{mea} - T_{cal})^2}$$

where

N : Number of data

T_{mea} : Measurement

.

T_{cal} : Calculated result

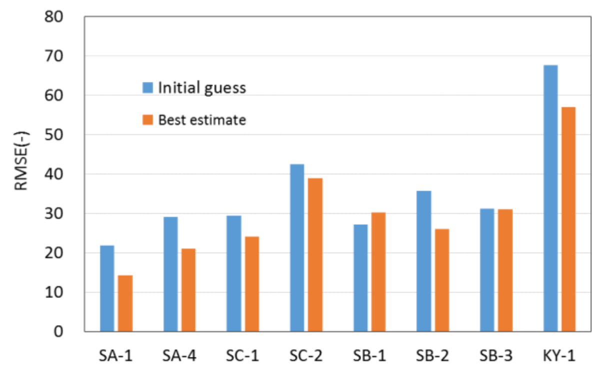

Fig 9: RMSE of simulated temperature using initial guess and best estimate

Figure 10 shows a comparison of simulated results and measurements for feed zone depth pressure in wellbores. The pressure profiles of the initial guess and the best estimate were almost the same, so we represented both pressures as “calculated” (Fig. 10). We evaluated the differences quantitatively using relative error (RE) as shown in Fig. 10 (right). The pressure profiles show a zone deeper than −200m a.m.s.l. However, there are discrepancies between the simulated and measured values in the shallow zone. RE is defined as:

$$RE = \frac{P_{mea} - P_{cal}}{P_{mea}}$$

where

P_{mea} : Measurement

P_{cal} : Calculated result (or simulated)

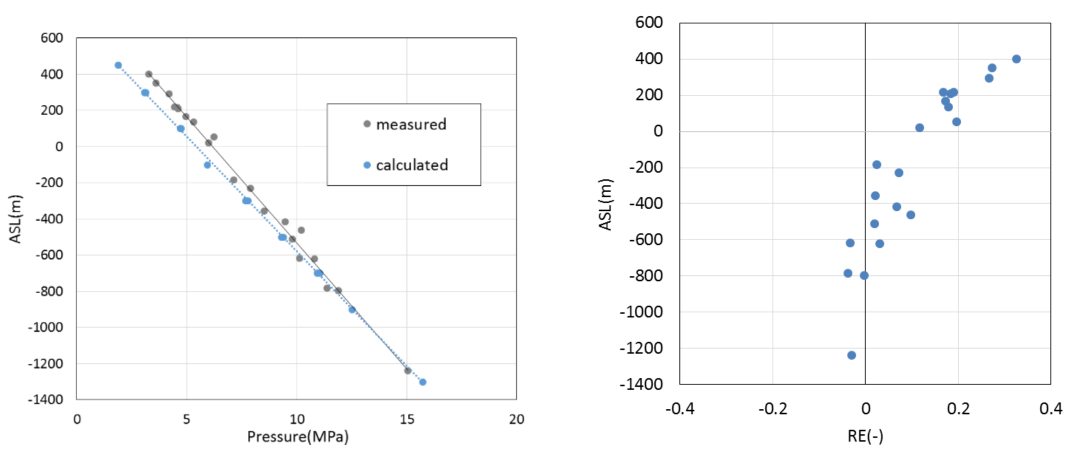

Figure 10: Comparison of simulated results and measurements for feed point pressure and relative error (RE)

3.2 Simulation results of the history matching

Figure 11 shows a comparison between calculated results and measurements for the specific enthalpy of production wells in history matching simulation for 20 years. Orange circle and blue diamond indicate specific enthalpy measurement and simulated results of the initial guess, respectively. These figures also show production rates for each well for 20 years. A good match with measurements in low specific enthalpy cases such as Well S-4 was obtained. However, high specific enthalpy values in cases such as Well SA-4 could not be matched. This may be because that a steam-water two-phase region was not well formed in the simulated results.

Figure 11 also shows simulated results of specific enthalpy using permeabilities of the best estimate in the history matching simulation. Black triangles depict simulated results using best estimated permeabilities. Although the simulated result for specific enthalpy using the best estimate shows a higher specific enthalpy than the results obtained with the initial guess, these results still have large discrepancies with measurements for wells discharging high enthalpy fluid, especially Well SA-4. It is estimated that a two-phase region exists in these areas in Sumikawa. It is necessary to review pressure distribution because pressure distribution in the reservoir is important for generating a two-phase region. Figure 12 shows the vertical cross section of temperature profiles in W-E and N-S 20 years after production and injection activity begin. Low temperature zone indicated by concentric circles present the influence of reinjected water.

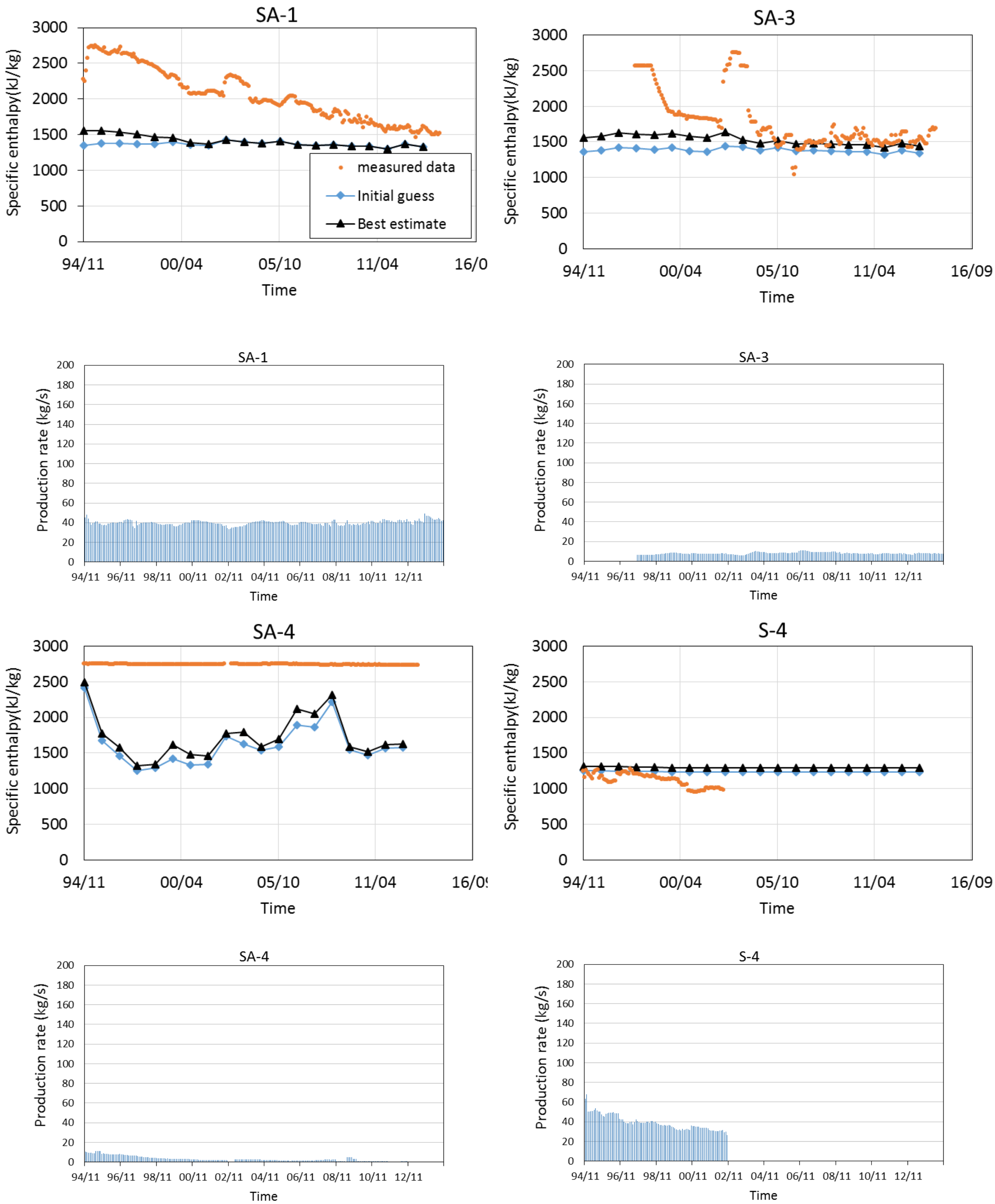

Figure 11: Specific enthalpy (before estimation, after estimation, and measurement) and production rate of each well

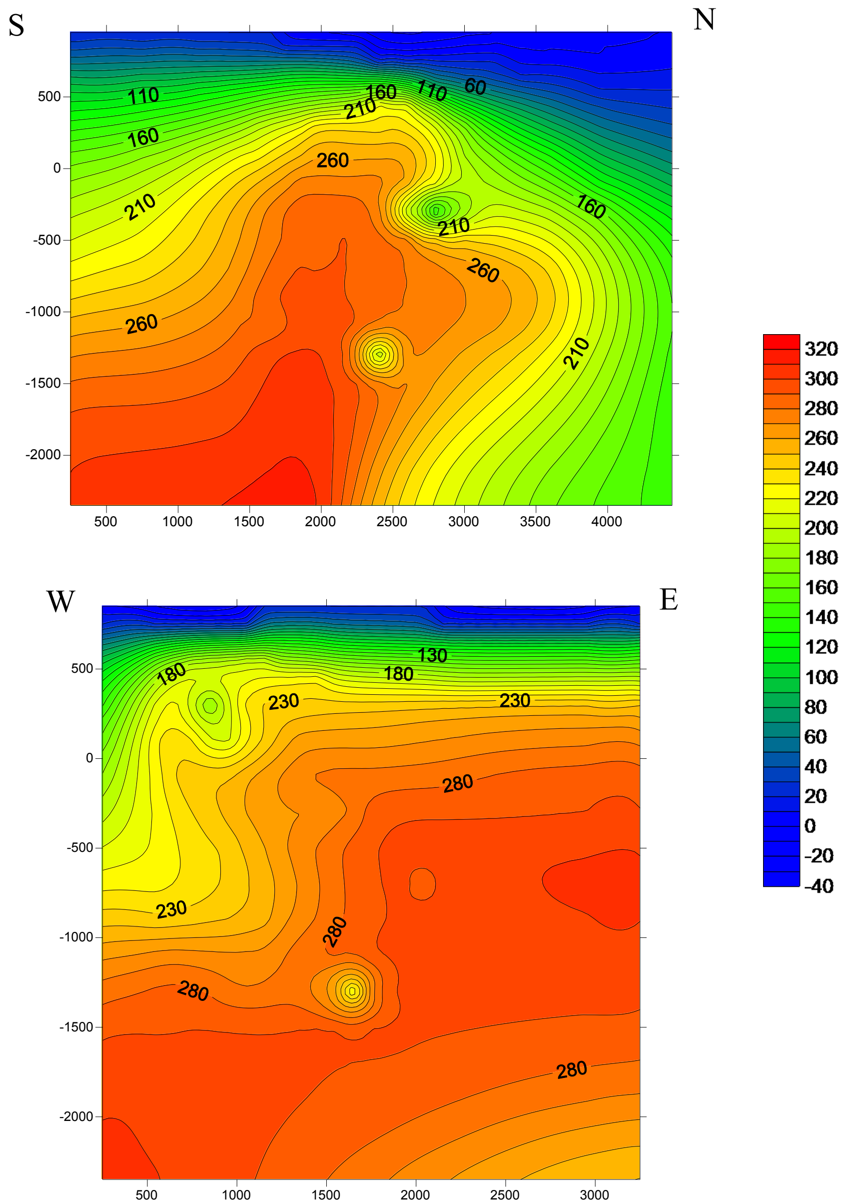

Figure 12: Cross section of temperature profiles in S-N and W-E 20 years after production and injection activity initiated

4. CONCLUSIONS

We developed a numerical model of the Sumikawa geothermal reservoir. We performed forward analysis, sensitivity analysis, and inversion analysis. Firstly forward analysis was performed to fit the results of the temperature profile of well with measurements by changing the parameters, mainly permeabilities. Secondly we performed a sensitivity analysis to identify the large sensitivity rock types. Thirdly using inversion analysis, we extracted parameters with a large sensitivity, and estimated unknown parameters (mainly permeabilities) for the natural state and history matching simulation using iTOUGH2. We estimated rock permeabilities from measured temperature and data in the natural state, and the specific enthalpy of the production fluid during production history. Then, we compared the simulated results with measurements for temperature and pressure distributions using RMSE and RE.

For inversion analysis, estimated parameters through forward analysis were given for the initial guess, then the best estimate was obtained. Inversion analysis with iTOUGH2 resulted in a decrease in RMSE, however the decrease in RMSE was in sufficient, and thus there is still room for improvement. In the history matching simulation using the best estimate, there was a small improvement. Simulated results indicated that it was difficult to reproduce properly model the high specific enthalpy zone in reservoir.

ACKNOWLEDGMENT

The authors thank Mitsubishi Materials Co. for its support and permission to use field data.

REFERENCES

Finsterle, S.: iTOUGH2 User's Guide, Report LBNL-40040 Updated Reprint, Earth Sciences Division, Lawrence Berkeley National Laboratory, University of California, Berkeley, CA 94720, (2000).

Kato, K.: Study on Modeling of Reservoir and Wellbore for Geothermal Reservoir Management, Faculty of Science and Engineering, Waseda University, Japan, doctoral thesis, (2003), 126-144.

Pruess, K., Oldenburg, C., and Moridis, G.: TOUGH2 User's Guide Version 2.0, Report LBNL-43134, Earth Sciences Division, Lawrence Berkeley National Laboratory, University of California, Berkeley, California 94720, (1999).

Thunderhead Engineering: PetraSim User Manual, (2016). https://www.rockware.com/assets/products/148/downloads/documentation/49/petrasimmanual.pdf (accessed 2016)